Iranian Journal of Science and Technology, Transactions of Civil Engineering (2019) 43:649–662
https://doi.org/10.1007/s40996-018-0223-z

RESEARCH PAPER

# Shape Optimization of Double-Arch Dams by Using Parameters Obtained Through Bayesian Estimators

**Enrico Zacchei**[1] · **José Luis Molina**[1]

Received: 19 December 2017 / Accepted: 12 December 2018 / Published online: 18 December 2018


**Abstract**
The aim of this paper is to define the optimum shape of double-arch dams. This is studied here considering the shape of existing double-arch dams located in Spain. The analysis has been carried out in two consecutive stages. The first one refers to defining issues about Bayesian estimators to obtain the value for designing the optimum dam shape. In the second stage, the shape equations are iterated step-by-step. Data are taken from the inventory of Spanish existing dams. To obtain the non-available data, the Gaussian distribution under the Bayesian theorem hypotheses has been employed. This theorem converts the prior distribution using unknown parameters into the posterior distribution which provides expected parameters, i.e. the Bayesian estimators. The main challenge of the analysis is to identify the parameters which define the optimum shape of an existing dam. For this, over 30 dams have been selected and over 700 data have been collected. One of the main practical implications of this research comprises a reduction of the concrete volume, which implies a reduction of the financial costs and the environmental impact.

**Keywords** Shape optimization · Bayesian estimators · Double-arch dams · Spanish dams

## 1 Introduction

The main goal of this paper is to define an optimum shape for double-arch dams. This has been developed by considering and analysing the existing double-arch dams located in Spain. From the inventory of existing dams, one can notice a great range of data; however, some important ones are not available. To estimate the non-available data, the Bayesian theorem has been adopted here. In this analysis, 34 double-arch dams have been identified, of which 11 were built over 50 years ago.

The objective of optimizing double-arch dams through mathematical modelling is not only to make explicit the scheme of optimum design under certain conditions, but also to minimize the discrepancy between the simulated data and the collected data.

✉ Enrico Zacchei
enricozacchei@usal.es

José Luis Molina
jlmolina@usal.es

[1] Higher Polytechnic School of Ávila, University of Salamanca (USAL), 50, Avenue Hornos Caleros, 05003 Ávila, Spain

The shape design of double-arch dams is based on the experience of the designer and on the following techniques: modelling, analysis, testing the materials to avoid defects and accuracy analysis of the error corrections to avoid inadequate constructions. The decrease of uncertainties largely comprises a mix of experience, best practice, prudent estimation of material properties and utilization of a conservative approach to modelling. Given that this is a field that mainly relies on the engineers' experience and innovative methods carried out by researches, the gap between engineering practice and engineering research should be reduced.

Double-arch dams are one of the most important challenges in designing and modelling. They are usually a topic of research—by using drones (Ridolfi et al. 2017; Buffi et al. 2017a, b) and sensors (Zhu et al. 2016; Reinoso et al. 2017) as innovative methods—as they have several purposes for society, economic growth and urban economization, for example water supply, flood control, irrigation of local agriculture, navigation or hydropower generation.

Dam safety has gained increasingly more attention due to the considerable damage (high risk) that may occur when accidents and failures happen. Defining information regarding safety and economy in the design of arch dams

is an issue that has been studied for many years (Savage and Houk 1931).

Moreover, dams are multihazard-vulnerable structures (Yuen 2010; Yuen et al. 2006) affected by phenomena such as earthquakes (Baker and Gupta 2016), flooding and stability of terrain, to name a few examples. Some causes of failures are the foundation deterioration (aging phenomena), water overtopping, debris that block the spillways, piping cracks, uplift pressures higher than design pressures, high temperature during the construction (Zhang et al. 2015) or non-uniform temperature due to the solar radiation (Jin et al. 2010). Therefore, for all types of dams, monitoring to avoid cracks (Li et al. 2013) and geophysical inspections (Cardarelli et al. 2010, 2014) are of primary importance.

Engineers need to combine the traditional analysis with risk assessment approach to obtain a good understanding of the expected structure performance and its risk.

The geometric shape of double-arch dams is the main factor that influences their own stability. In addition, it affects the project cost. The cost of double-arch dams largely includes the concrete volume and the area and the foundation excavation (Akbari et al. 2011; Fan et al. 2015).

In the literature, there are some interesting cases that optimize the arch dam shape, for example, using complex methods (Xiao-fei et al. 2009; Shouyi et al. 2009), genetic algorithms (Seyedpoor and Gholizadeh 2008) (for earth dams see Li et al. (2016)) and combining approaches relating other methods (Seyedpoor et al. 2011). There are also other optimization methods which are used to define the material parameters (Gu et al. 2015). For concrete gravity dams, the optimal shape including the interaction dam–water foundation has been studied in (Khatibinia and Khosravi 2014; Khosravi and Heydari 2013) idealizing the dam as the triangular shape in the 2D analysis.

To design dams, there are some limitations imposed by topographic and geologic conditions. A lack of knowledge on shear strength parameters in the dam–foundation interface can be very dangerous for dam safety (Alrarejos-García et al. 2015). Most dams are built on rocky foundation but some are built on foundation with very low deformation modulus, such as the Vajont Dam, situated in Italy, and the Mauvoisin Dam in Switzerland (Fan et al. 2015). The deformability of the foundation can considerably increase the stresses in the dam body. Obviously, an advanced geological survey must be conducted before construction to avoid such problems.

The geometry of cantilevers and arches defines the dam shape and, consequently, the distribution and magnitude of the stresses. In the dam shape optimization analysis, several kinds of stresses should be considered as constraints. In particular, the constraints could be defined in terms of allowable tensile and compressive stresses in the cantilevers and in the upstream–downstream face of dam blocks.

The Bayesian theorem is employed to convert the prior distribution of uncertainty parameters into the posterior distribution by using the gathered data. The Bayesian statistical framework is of great interest in the civil engineering research field, especially for structural models based on numerous data and parameters that are difficult to obtain otherwise (Beck and Katafygiotis 1998; Conte et al. 2015).

For example, the option to use the Bayesian theorem to calculate the unknown parameters to define the geometry of double-arch dams results from an analysis of Bartoli et al.'s work (2017). Here, the Bayesian theorem has been used to obtain the parameters as the elastic modulus and the structural period, which are usually uncertain parameters.

The first part of the paper presents materials and methods to show the data. The second part presents the geometrical model and their design constraints and optimization criteria. Then, the Bayesian estimators are defined, and finally the analysis and results are shown. The mathematical programme Wolfram Mathematica (2017) is used here, which overcomes the flaws of complex integrations and has a great work capacity and high efficiency.

## 2 Materials and Methods

This section shows the general methodology to define the shape optimization of double-arch dams by using appropriate equations. To define the variables of the problem, the Bayesian method has been used; its general methodology has also been shown.

The shape optimization process requires careful availability of existing dam's data, body shape modification, adequate structural design, evaluation of the constraints and feedback analysis in relation to the standard design criteria. Finding the optimal shapes of double-arch dams means optimizing the cost, too.

The Bayesian method is a stochastic method that can be interpreted as a series of logical multi-values for plausible reasoning under incomplete information. A probability distribution gives a measure of how plausible each variable is. The evaluation of uncertainties plays an important role in the analysis of the constructed facility. The type of uncertainty or aleatory variable cannot be eliminated but it can be estimated and, therefore, reduced.

Figure 1 shows the architecture of the planned methodology for optimization of double-arch dams. The procedure of the flowchart is explained as follows (the equations and the variables are explained in detail in the successive sections): firstly, the inventory data of double-arch dams in Spain and other data from the literature are collected. Then, the equations of the horizontal section shape (up- and downstream face) of double-arch dams are written by using a programme Wolfram Mathematica (2017). The equation about the radii

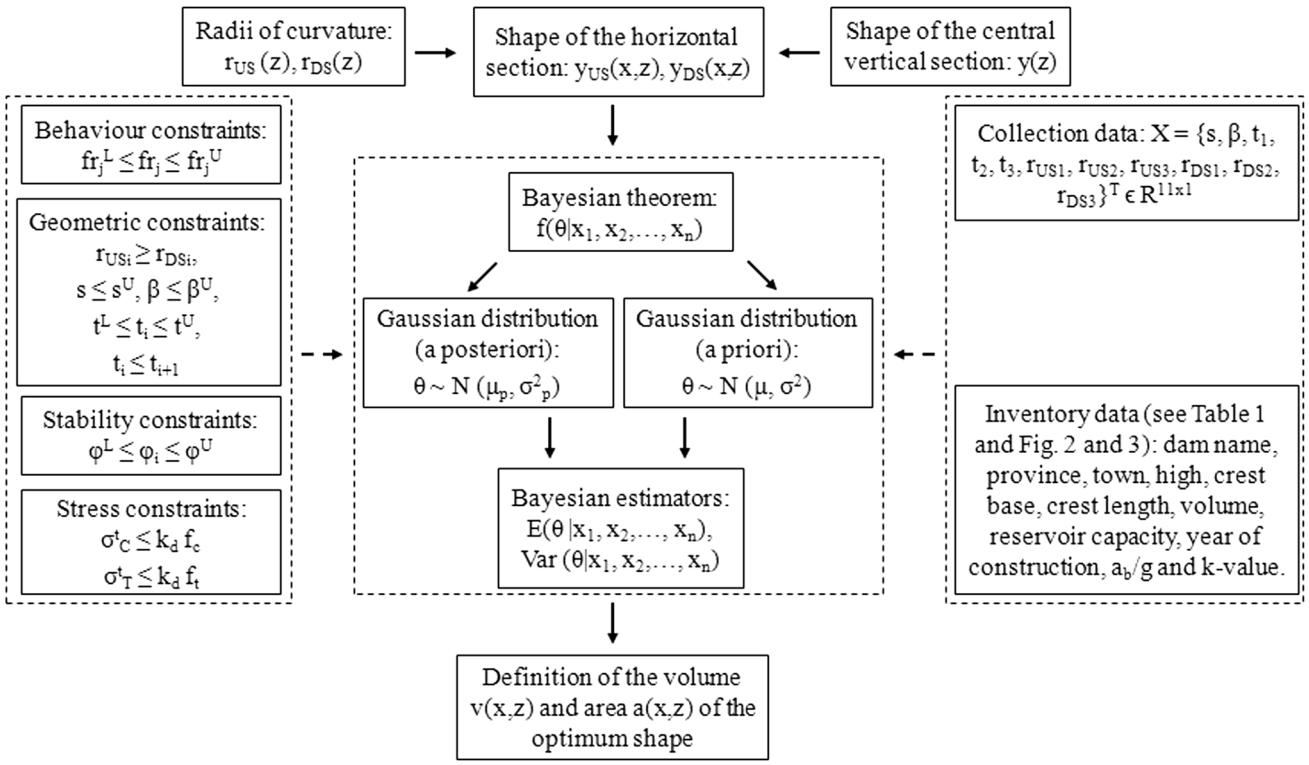


**Fig. 1** Flowchart of the study methodology

of curvature and the equation of the central vertical section are included in the first ones. After that, the Gaussian distribution (a priori and a posteriori) is defined under the hypothesis of the Bayesian theorem and the Bayesian estimators are calculated. Finally, the verification of values consistent with the adopted constraints takes place, and consequently, the volume and area of the optimum shape of the dam are defined.

Table 1 shows the inventory of the data of double-arch dams that have been analysed in this work. The selection criteria are: (1) height of the double-arch dam > 35.0 m and (2) sufficiently available information to carry out the analysis. Some values of the crest base dams are not available. Data to build the inventory are available online (SEPREM 2017; SNCZI 2017). An intersection of data available on the websites has been made to reach more complete information.

Data about the location (province and city) and purpose (use of reservoir) help to collocate the optimum dam in a more detailed context. However, it is important to highlight that the results refer to an ideal dam; therefore, a specific context is difficult to identify.

Figures 2 and 3 show dams that are based on the ground basic acceleration $a_b$ and $k$ value (coefficient of contribution), which considers the influence of the different types of earthquakes expected in the seismic hazard of each point. Some values of the $a_b/g$ and $k$ are not available in the Spanish code (NCSE-02 2002); therefore, they have been estimated. The mean value of the dams' height, in Table 1, is used to carry out the mathematical analysis. This deterministic value (95.55 m) is compatible—in accordance with the inventory (Table 1) and literature (USACE 1994)—with different factors (i.e. crest length and central angle of dam, which are explained later).

In Fig. 2, it is possible to note that the higher value occurs for the Beznar Dam (186.4 cm/s$^2$) and the Quentar Dam (196.2 cm/s$^2$) which are in Granada province in the Andalusian region (southern Spain). In fact, in this region the seismic intensity is relevant (IGN-UPM 2013). Considering all data, the mean acceleration is 56.9 cm/s$^2$. The $k$ value considers the different earthquakes' type, for example distant and strong earthquakes or near and weak ones. It is possible to note, in Fig. 3, that these values are rarely considered, i.e. $k = 1.0$; as it is very difficult to standardize the seismic activity, it is always necessary to do a specific study "in situ".

## 3 Geometrical Model Theory

The shape of dams relates to the local building materials and construction techniques. The double-arch dams with various thickness measures are usually chosen. The geometrical model must be analysed in two perspectives: in a vertical and

**Table 1** Inventory of double-arch dams in Spain

| Dam name | Province | City | Height (m) | Crest base (m) | Crest length (m) | Volume ($10^3$ m) | Reservoir capacity (h $m^3$) | Year of construction | Use of reservoir |
|---|---|---|---|---|---|---|---|---|---|
| Albarellos | Orense | Leiro y Boboras | 90.00 | 3.00 | 285.00 | 217.00 | 90.70 | 1971 | H |
| Alloz | Navarra | Yerri, Guesalaz | 66.80 | 1.50 | 74.40 | 18.47 | 65.31 | 1930 | H/I |
| Almendra | Salamanca | Almendra y Villar del Buey | 202.00 | 10.00 | 567.23 | 2.186 | 2648.64 | 1970 | H |
| Angeles, Los | Segovia | Vegas de Matute | 37.25 | ? | 110.00 | 5.70 | 1.76 | 1969 | R |
| Atazar, El | Madrid | Patones y Atazar | 134.00 | 8.00 | 484.00 | 1100.00 | 425.00 | 1972 | W |
| Baells, La | Barcelona | Berga | 102.35 | ? | 302.38 | 400.00 | 109.43 | 1976 | W/H |
| Barca, La | Asturias | Tineo y Belmonte | 74.00 | 4.00 | 178.00 | 113.00 | 31.10 | 1966 | H |
| Baserca | Huesca | Montanuy, Vilaller | 86.00 | 8.00 | 330.00 | 230.00 | 21.86 | 1983 | H/F |
| Belesar | Lugo | Chantada | 129.00 | 5.50 | 500.00 | 735.00 | 654.10 | 1963 | H |
| Beznar | Granada | Pinar, El | 134.00 | 7.50 | 408.00 | 485.00 | 53.60 | 1986 | W/H |
| Canelles | Huesca | Estopiñan del Castillo, Os de Balaguer | 151.00 | 6.00 | 210.00 | 332.994 | 678.00 | 1960 | H |
| Castro de las Cogotas | Avila | Cardeñosa/ Avila | 67.00 | ? | 299.20 | 117.30 | 58.70 | 1994 | W/H |
| Cohilla, La | Cantabria | Tudanca | 116.00 | 2.00 | 288.00 | 181.00 | 11.80 | 1950 | H |
| Eiras | Pontevedra | Fornelos de Montes | 51.00 | 2.00 | 191.00 | 46.70 | 22.17 | 1977 | W |
| Eume | La Coruña | Capela, A, Monfero | 103.00 | 3.20 | 284.00 | 225.00 | 123.00 | 1960 | H |
| Guara | Huesca | Casbas de Huesca | 63.00 | 4.50 | 85.00 | 13.746 | 3.65 | 1995 | W/I |
| Guijo de Granadilla | Caceres | Guijo de Granadilla | 51.50 | 5.00 | 210.00 | 95.41 | 13.00 | 1982 | H |
| Jose Toran | Sevilla | Lora del Rio | 77.00 | 8.50 | 362.00 | 206.15 | 101.24 | 1992 | W/I |
| Lanuza | Huesca | Sallent de Gallego | 79.60 | 3.00 | 176.33 | 65.08 | 25.00 | 1978 | H |
| Llauset | Huesca | Montanuy | 89.00 | 7.10 | 300.00 | 220.00 | 16.78 | 1983 | H |
| Llosa del Cavall, La | Lleida | Naves | 122.00 | 8.00 | 326.00 | 350.00 | 79.40 | 1999 | W/F |
| Matalavilla | Leon | Paramo del Sil | 115.00 | 2.50 | 240.00 | 170.00 | 60.74 | 1967 | H |
| Montejaque | Malaga | Montejaque | 83.75 | 3.00 | 84.00 | 30.00 | 36.00 | 1924 | H |
| Pedrezuela (Vellon, El) | Madrid | Pedrezuela | 52.50 | ? | 218.00 | 95.00 | 41.23 | 1967 | W |
| Ponton Alto | Segovia | Palazuelos de Eresma, San Ildefonso | 49.00 | ? | 248.00 | 92.69 | 7.41 | 1993 | W |
| Portas, Las | Orense | Vilariño de Conso | 141.00 | 9.00 | 476.70 | 641.00 | 535.70 | 1974 | H |
| Quentar | Granada | Quentar | 133.00 | 3.50 | 200.00 | 227.00 | 13.60 | 1975 | W/I |

**Table 1** (continued)

| Dam name | Province | City | Height (m) | Crest base (m) | Crest length (m) | Volume ($10^3$ m) | Reservoir capacity (h $m^3$) | Year of construction | Use of reservoir |
|---|---|---|---|---|---|---|---|---|---|
| Quiebrajano | Jaen | Valdepeñas de Jaen, Campillo Arena | 71.50 | 5.50 | 212.00 | 119.92 | 31.60 | 1976 | W |
| Riaño | Leon | Cremenes | 100.50 | 4.20 | 337.40 | 270.00 | 664.00 | 1988 | H/I |
| Santa Eulalia | Orense | Veiga, La, Bollo | 73.00 | 5.00 | 212.00 | 72.40 | 11.00 | 1966 | H |
| Soria | Las Palmas | San Bartolome de Tirajana | 132.00 | ? | 148.45 | 211.68 | 32.30 | 1972 | W/H |
| Susqueda | Gerona | Susqueda | 135.00 | 5.00 | 510.00 | 662.00 | 233.00 | 1968 | W/H |
| Tajera, La | Guadalajara | Sotillo, El | 39.00 | 4.50 | 220.11 | 67.00 | 9.94 | 1973 | I/F |
| Valdecañas | Caceres | Belvis de Monroy y Cañas de Tajo | 98.00 | 2.50 | 290.00 | 270.00 | 1446.00 | 1964 | H/I |

*H* hydroelectric generation, *I* irrigation, *W* water storage, *R* recreation, *F* flood control

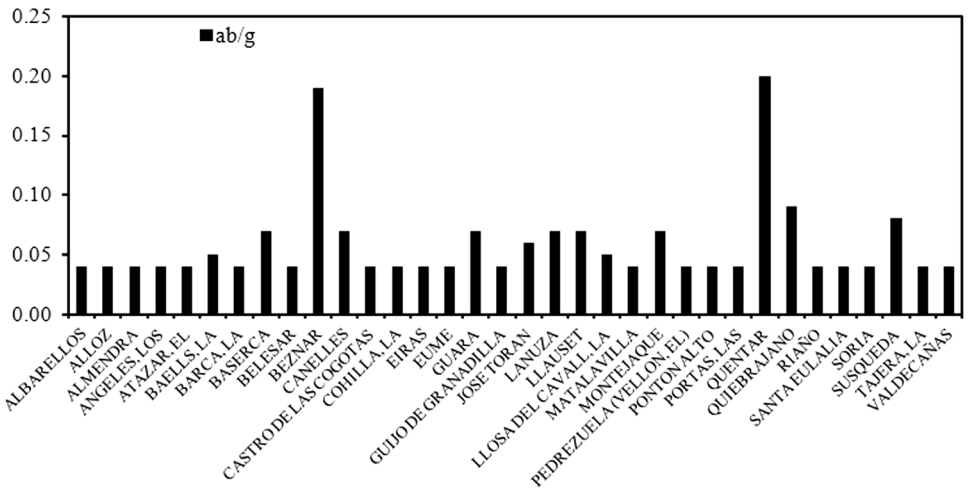


**Fig. 2** Seismic accelerations $a_b/g$ for each studied dam

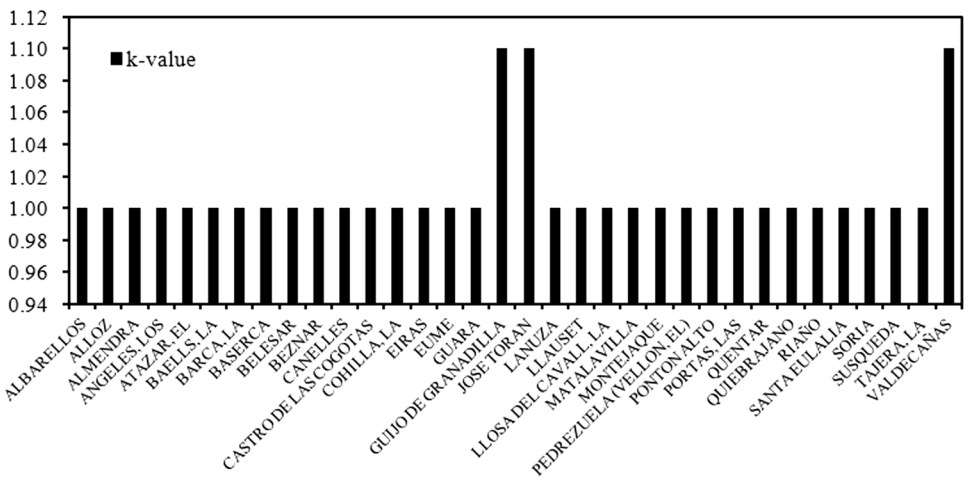


**Fig. 3** Coefficient *k* for each studied dam

in a horizontal section. For the vertical section, it is possible to consider the central section because this is in general greater than the other sections, whereas the horizontal section should be considered as a parabolic curve. The dam site can be considered symmetrical at a large scale.

However, it is important to know that the dams can have different curvature centres (or planes of centres) and therefore different laws for the upstream (US) and downstream (DS) faces at $z$-axis. For example, one plane of centres is used to describe arches in a symmetrical site, whereas two planes of centres or more are used to describe arches in non-symmetrical sites USACE (1994).

Dams are formed by cantilevers and arches. The behaviour of cantilevers is idealized as a beam, and the crown cantilever is the highest beam of the dam. The studied structure is double-curved; it is symmetrical in plant with respect with the main section and placed on a base (foundation) which extends all around the perimeter of the abutments. The US and DS faces increase the thickness of the cantilevers progressively, collaborating with the dam stability during the construction.

The external loads, acting on the dam body and abutments, increase as the dam's depth increases and problems such as high slope stability arise.

The main parameters that describe the geometric shape are the US curve $y_{US}(x, z)$, the DS curve $y_{DS}(x, z)$, thickness of cantilevers $t(z)$, the outside $r_{US}(z)$ and inside $r_{DS}(z)$ radius of the horizontal arch ring and the function that defines the vertical section $y(z)$. Figure 4 shows the vertical and horizontal section of a double-arch dam.

The geometrical model of a double-curvature arch dam is based on Kaveh and Ghaffarian's work (2014). A polynomial of second order is considered to define the shape of the central vertical section for the curve of the US face. The function is defined by:

$$y(z) = -sz + \frac{sz^2}{2\beta h} \tag{1}$$

where $s$ is the slope at crest, $h$ is the height of the dam and $\beta = z/h$.

The equations that define the shape of the horizontal section at the US and DS faces of the dam are:

$$y_{US}(x, z) = \frac{1}{2r_{US}(z)}x^2 + y(z) = \frac{1}{2r_{US}(z)}x^2 - sz + \frac{sz^2}{2\beta h} \tag{2}$$

$$y_{DS}(x, z) = \frac{1}{2r_{DS}(z)}x^2 + y(z) + t(z) = \frac{1}{2r_{DS}(z)}x^2 - sz + \frac{sz^2}{2\beta h} + t(z) \tag{3}$$

where $r_{US}$ and $r_{DS}$ are the radii of curvature of the US and DS curves, respectively. In Eq. (3), the thickness of the central vertical section is expressed as:

$$t(z) = \sum_{i=1}^{n+1} L_i(z)t_i \tag{4}$$

where the Lagrange interpolation function associated with the $i$th ($i = 1, 2, \ldots, n+1$) level can be defined (with $k \neq i$ to avoid the denominator being zero) as:

$$L_i(z) = \frac{\prod_{k=1}^{n+1}(z - z_k)}{\prod_{k=1}^{n+1}(z_i - z_k)} \tag{5}$$

where $z_i$ denotes the $z$-axis of the $i$th level in the central vertical section, and $n$ is the segments of the dam which have been chosen as 2 in this analysis; i.e. the dam is divided into

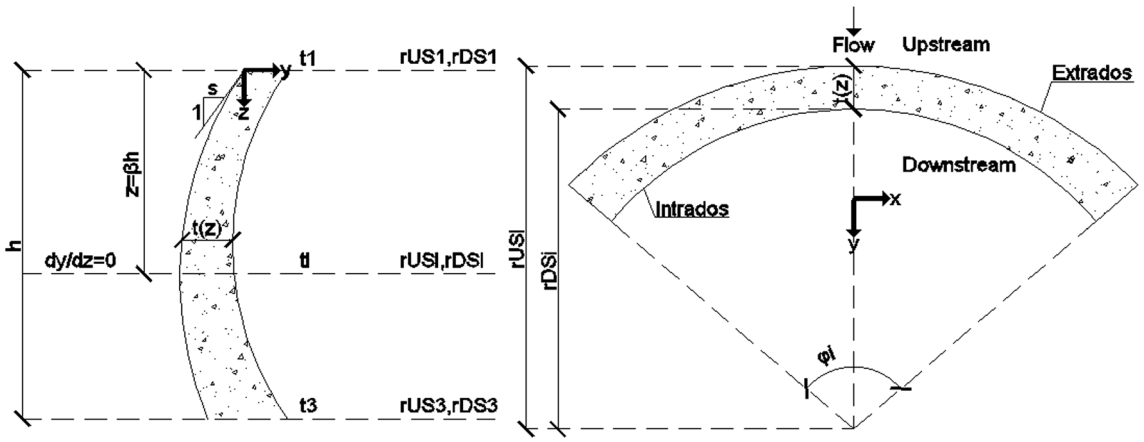


**Fig. 4** Vertical (left) and horizontal (right) section of a double-arch dam (AutoCAD 2010). Where: $h$ = height; $s$ = slope; $r_{USi}$ = radii of curvature of the US at the $i$th level; $r_{DSi}$ = radii of curvature of the DS; $t_i$ = thickness; and $\varphi_i$ = central angle. The orientation of the axis is: $y$-axis (US-DS), $x$-axis (left side-right side) and $z$-axis (top–bottom)

two vertical and horizontal segments. The radii of curvature are defined by:

$$r_{\mathrm{US}}(z) = \sum_{i=1}^{n+1} L_i(z) r_{\mathrm{US}i} \tag{6}$$

$$r_{\mathrm{DS}}(z) = \sum_{i=1}^{n+1} L_i(z) r_{\mathrm{DS}i} \tag{7}$$

with $r_{\mathrm{USi}}$ and $r_{\mathrm{DSi}}$ as the values of $r_{\mathrm{US}}$ and $r_{\mathrm{DS}}$ at the $i$th level, respectively.

### 3.1 Design Constraints

To model the dam shape, constraints $g_{(\cdot)}(X)$ must be considered. Constraints refer to the behaviour, geometry, stability and stresses of dams. The design constraints have been taken in Saber Mahani et al.'s work (2015). Some design layout and general design considerations have been added in accordance with the technical manual USACE (1994).

The constraints related to the dam behaviour are defined as follows (for $j = 1, 2, \ldots, n_j$):

$$\mathrm{fr}_j^{\mathrm{L}} \le \mathrm{fr}_j \le \mathrm{fr}_j^{\mathrm{U}} \Rightarrow g_{bj}^{\mathrm{L}}(X) = 1 - \frac{\mathrm{fr}_j}{\mathrm{fr}_j^{\mathrm{L}}} \le 0; \quad g_{bj}^{\mathrm{U}}(X) = \frac{\mathrm{fr}_j}{\mathrm{fr}_j^{\mathrm{U}}} - 1 \le 0 \tag{8}$$

where $\mathrm{fr}_j$, $\mathrm{fr}_j^{\mathrm{L}}$ and $\mathrm{fr}_j^{\mathrm{U}}$ are the natural frequency and the lower and upper bounds on $j$th natural frequency, respectively; $n_j$ is the number of natural frequencies. The natural frequency of dams is influenced by reservoir, sediments and foundation interaction. Usually, for the whole system (dam–reservoir–foundation–sediment), the natural frequency is lower than the natural frequency for a single dam. The range of the fundamental structural period can be considered, for a single dam, 0.25–0.35 s (2.86 Hz $\le \mathrm{fr}_1 \le$ 4.0 Hz). For the whole system, it is possible to consider $\mathrm{fr}_1 \ge 3.33$ Hz.

In this analysis, the rock mass is not considered, only the stiffness (stiffness $\rightarrow \infty$) is included; in this case, the natural frequencies (dam + foundation) are very close to those of the dam alone. Moreover, the natural frequencies strongly depend on the materials' mechanical properties (e.g. elastic modulus), which can influence the dynamic response.

The geometric constraints refer to the design of the curvature radii, slope and thickness of the central vertical section. The constraint about the curvature radii prevents the intersection of the DS and US faces; this constraint is defined as:

$$r_{\mathrm{DS}i} \le r_{\mathrm{US}i} \Rightarrow g_{gci}(X) = \frac{r_{\mathrm{DS}i}}{r_{\mathrm{US}i}} - 1 \le 0 \tag{9}$$

where $r_{\mathrm{DSi}}$ and $r_{\mathrm{USi}}$ are the curvature radii of the DS and US faces of the dam in $i$th position in $z$-axis direction. The central lines of the curvature's radii change according to the height. The radius of the dam axis $r_{ai}$ defined by $r_{\mathrm{a}i} = r_{\mathrm{US}i} - (t_i/2)$ can be estimated as 0.6 of the straight-line distance at the top measured between the abutments ($l_{\mathrm{a}}$). In order to construct it easily, the constraint of the curve slope in the central section at crest level is defined as:

$$s \le s^{\mathrm{U}} \Rightarrow g_{gs}(X) = \frac{s}{s^{\mathrm{U}}} - 1 \le 0 \tag{10}$$

where $s^{\mathrm{U}}$ is the allowable maximum value of the slope. It is also possible to consider one slope at the foundation level having two types of slopes. However, in this analysis, only one slope has been considered. Besides the slope, $\beta$-value must be considered: $g_{g\beta}(X) = (\beta/\beta^{\mathrm{U}} - 1) \le 0$. In this analysis, the values $s^{\mathrm{U}}$ and $\beta^{\mathrm{U}}$ have been defined as 0.36 and 1.0, respectively. Other geometric constraints refer to the thickness defined as:

$$t^{\mathrm{L}} \le t_i \le t^{\mathrm{U}} \Rightarrow g_{gt}^{\mathrm{L}}(X) = 1 - \frac{t_i}{t^{\mathrm{L}}} \le 0; \quad g_{gt}^{\mathrm{U}}(X) = \frac{t_i}{t^{\mathrm{U}}} - 1 \le 0 \tag{11}$$

where $t^{\mathrm{L}}$ and $t^{\mathrm{U}}$ are the lower and upper values of the thickness of the central vertical section, respectively. To achieve the acceptable shape of double-arch dams, at different levels, this must be verified:

$$t_i \le t_{i+1} \Rightarrow g_{gt}(X) = \frac{t_i}{t_{i+1}} - 1 \le 0 \tag{12}$$

The stability constraints of abutments depend on: (1) the stability safety coefficient of the dam's abutment masses sliding, (2) the thrust angle constraint of the arch abutments and (3) the central angle constraint of the arch rings. When the rock mass condition of the dam abutments is relatively good, the central angle of the arch rings should have large intervals, and the optimal central angle can be selected according to stress constraints. The constraints that govern the stability of the structure may be expressed as:

$$\varphi^{\mathrm{L}} \le \varphi_i \le \varphi^{\mathrm{U}} \Rightarrow g_{si}^{\mathrm{L}}(X) = 1 - \frac{\varphi_i}{\varphi^{\mathrm{L}}} \le 0; \quad g_{si}^{U}(X) = \frac{\varphi_i}{\varphi^{\mathrm{U}}} - 1 \le 0 \tag{13}$$

where $\varphi^{\mathrm{L}}$ and $\varphi^{\mathrm{U}}$ are the central angle of the dam for DS and US levels in $i$th level, respectively, and $\varphi_i$ is the central angle of the arch dam. The central angle, defined by Eq. (13), also equilibrates the sliding between the blocks that form the dam. Equations (9)–(13) are valid for $i = 1, 2, \ldots, n+1$.

The largest practicable central angle should be used considering that the foundation topography may be inaccurately mapped and that the arch abutments may be extended to deeper excavation than originally planned. Due to limitations imposed by the topographic conditions and foundation requirements, for most layouts, $\varphi_i$ varies between 90° and 130°.

Finally, in order to ensure the dams safety during the construction and service, the maximum stress in the dam body has to be limited. The constraints about the stresses are defined by:

$$\begin{aligned} &\sigma_{\mathrm{C}}^{\mathrm{t}} \le k_{\mathrm{d}} f_{\mathrm{c}} \le g_{Cm}(X,t) = \frac{\sigma_{\mathrm{C}}^{\mathrm{t}}}{k_{\mathrm{d}} f_{\mathrm{c}}} - 1 \le 0; \\ &\sigma_{\mathrm{T}}^{\mathrm{t}} \le k_{\mathrm{d}} f_{\mathrm{t}} \Rightarrow g_{Tm}(X,t) = \frac{\sigma_{\mathrm{T}}^{\mathrm{t}}}{k_{\mathrm{d}} f_{\mathrm{t}}} - 1 \le 0 \end{aligned} \tag{14}$$

for $t = 0, 1, \ldots, n_{\mathrm{t}}$ and $m = 1, 2, \ldots, n_m$; $n_m$ is the number of dam elements and $n_{\mathrm{t}}$ is the earthquake duration; $\sigma_{\mathrm{C}}^{\mathrm{t}}$ and $\sigma_{\mathrm{T}}^{\mathrm{t}}$ are the principle compression and tension stresses in time $t$, respectively; $f_{\mathrm{c}}$ and $f_{\mathrm{t}}$ are the compressive and tensile strength for concrete, respectively; $k_{\mathrm{d}}$ is the incremental coefficients related to the effect of the dynamicity of loads.

Table 2 shows the summary of the constraints.

It is important to emphasize that the geometry, stability, behaviour and stress state are closely related to each other for these following reasons: (1) the central angle of the top arch is a controlling value which influences the curvature of the whole dam: tensile stresses will develop in arches of insufficient curvature. The geometry of the cantilevers and arches controls the dam shape and, as a consequence, the distribution and magnitude of the stresses; (2) the stresses near the rock surface depend on the central angle which is related to the angle between the arch thrust and the rock contour line. This angle must be greater than 30° to avoid high concentration of shear stresses near the rock surface; (3) the dam geometry should be consistent with the stress state of the dam and simple to facilitate construction; and (4) the stresses in the dam body are generated from the combinations of the following loads (for dynamic and static analysis) that influence the system behaviour: deadweight of dam + US water level + DS water level + vertical hydraulic force + silt pressure + temperature + uplift pressure + ice + post-tension + floating debris + applied force + horizontal force.

### 3.2 Optimization Criteria

Considering the different types of constraints illustrated in the previous section, it is possible to define the design variables of the mathematical problem, that is: $X = \{s, \beta, t_1, t_2, t_3, r_{\mathrm{US1}}, r_{\mathrm{US2}}, r_{\mathrm{US3}}, r_{\mathrm{DS1}}, r_{\mathrm{DS2}}, r_{\mathrm{DS3}}\}^{\mathrm{T}} \in R^{11x1}$. The mathematical problem is to find the components of the vector $X^{\mathrm{T}}$ and to optimize the volume and the area of the double-arch dams subjected to: $g_{(\cdot)}(X) \le 0$, where $X^{\mathrm{L}} \le X \le X^{\mathrm{U}}$, where $g_{(\cdot)}(X)$ is a number of inequality constraints; $X^{\mathrm{L}}$ and $X^{\mathrm{U}}$ denote the lower and upper bounds of the design variable vector, respectively. The volume $v(x, z)$ and the area $a(x, z)$ of the double-arch dams can be determined by integrating dam surfaces:

$$v(x,z) = \iint\limits_{\text{area}} \left| y_{\mathrm{DS}}(x,z) - y_{\mathrm{US}}(x,z) \right| \mathrm{d}x\mathrm{d}z \tag{15}$$

$$\begin{aligned} a(x,z) = &\iint\limits_{\text{area}} \sqrt{1 + \left(\frac{\mathrm{d}y_{\mathrm{US}}}{\mathrm{d}x}\right)^2 + \left(\frac{\mathrm{d}y_{\mathrm{US}}}{\mathrm{d}z}\right)^2}\, \mathrm{d}x\mathrm{d}z \\ &+ \iint\limits_{\text{area}} \sqrt{1 + \left(\frac{\mathrm{d}y_{\mathrm{DS}}}{\mathrm{d}x}\right)^2 + \left(\frac{\mathrm{d}y_{\mathrm{DS}}}{\mathrm{d}z}\right)^2}\, \mathrm{d}x\mathrm{d}z \end{aligned} \tag{16}$$

with $a(x, z) = a_{\mathrm{US}}(x, z) + a_{\mathrm{DS}}(x, z)$, the sum of areas of the up- and downstream faces, where $a_{\mathrm{US}}(x, z)$ and $a_{\mathrm{DS}}(x, z)$ are the area of up- and downstream faces, respectively, and $|\cdot|$, in Eq. (15), denotes the absolute value (nonnegative value). The region of integration called "area", in Eqs. (15) and (16), is produced by projecting the dam on $xz$ plane. The objective function that should be optimized is the sum of the $v(x, z)$ and $a(x, z)$.

## 4 Bayesian Estimators

The ability of the Bayesian technique is that it can be used to develop models whose data are insufficient due to the model complexity. Several variables must be used as samples, and the probability density function (PDF) must be defined.

It is always convenient to work using the Gaussian (or normal) distribution because it is easy to develop because it is only necessary to know its mean value and variance (or standard deviation) and its behaviour is well known. A Gaussian distribution is employed to consider the measurement errors when estimating variables.

Another ability is that when the mean value is unknown, it is possible to use a normal prior distribution: a distribution with a mean value supposed a priori. A normal distribution of this type is called prior distribution of Bayesian

**Table 2** Summary of the constraints

| Constraint | Definition | Equation |
|---|---|---|
| Behaviour | It considers the vibration frequency of the dam | Equation (8) |
| Geometric | It accounts the radii of curvature, slope and thickness of the dam | Equations (9)–(12) |
| Stability | It is defined by the central angle of the dam | Equation (13) |
| Stress | It depends on the compression and tension stresses of the dam | Equation (14) |

estimators (Ross 2008). To use the prior distribution, it is necessary to obtain some information about the random variables and to know their interval (maximum and minimum limit). Thus, a candidate value is estimated which can be the expected value.

As it was previously mentioned, to obtain the shape optimization of dams, it is necessary to define the design variables and their range, i.e. the lower and upper bounds. The Bayesian estimators have been used to define the variables $X = \{s, \beta, t_1, t_2, t_3, r_{US1}, r_{US2}, r_{US3}, r_{DS1}, r_{DS2}, r_{DS3}\}^T \in R^{11x1}$.

In this paper, a sample of 770 values have been taken, for example 70 values for each variable. Data have been collected from the literature (Kaveh and Ghaffarian 2014; Saber Mahani et al. 2015; Seyedpoor et al. 2010; Gholizadeh and Seyedpoor 2011; Hamidian and Seyedpoor 2010; Zacchei and Molina 2018). A large amount of data will be overwhelmed from results of the chosen initial PDF (a priori), and one can proceed using the predictive PDF (a posteriori) for the optimal model distribution.

The conditional density of the unknown parameter $\theta$ given the values $\{x_1, x_2, \ldots, x_n\}$, where $n$ is the number of the sample, is expressed by:

$$f(\theta|x_1, x_2, \ldots, x_n) = \frac{f(x_1, x_2, \ldots, x_n|\theta)p(\theta)}{f(x_1, x_2, \ldots, x_n)} \tag{17}$$

where the PDF a priori is defined by:

$$p(\theta) = \frac{1}{\sqrt{2\pi}\sigma} e^{\left\{-\frac{(\theta-\mu)^2}{2\sigma^2}\right\}}. \tag{18}$$

Using the Bayesian theory, the expected value (more probable) a posteriori and the variance a posteriori are defined, respectively, by:

$$E(\theta|x_1, x_2, \ldots, x_n) = \mu_p = \frac{n/\sigma_0^2}{n/\sigma_0^2 + 1/\sigma^2}\bar{x} + \frac{1/\sigma^2}{n/\sigma_0^2 + 1/\sigma^2}\mu \tag{19}$$

$$\mathrm{Var}(\theta|x_1, x_2, \ldots, x_n) = \sigma_p^2 = \frac{1}{n/\sigma_0^2 + 1/\sigma^2} \tag{20}$$

where $\sigma_0^2$ and $\bar{x}$ are the known variance and the sample mean, respectively.

The calculated PDF in this work concerns all the variables of the vector $X^T$; therefore, Eq. (17) becomes: $f(\theta|s, \ldots, n)$, $f(\theta|\beta, \ldots, n)$, $f(\theta|t_1, \ldots, n)$, $f(\theta|t_2, \ldots, n)$, $f(\theta|t_3, \ldots, n)$, $f(\theta|r_{US1}, \ldots, n)$, $f(\theta|r_{US2}, \ldots, n)$, $f(\theta|r_{US3}, \ldots, n)$, $f(\theta|r_{DS1}, \ldots, n)$, $f(\theta|r_{DS2}, \ldots, n)$ and $f(\theta|r_{DS3}, \ldots, n)$.

The concept of this study is the following: by changing the parameters $\{x_1, x_2, \ldots, x_n\}$, related to the shape of an existing dam, it is possible to estimate an optimal shape. In this sense, it is necessary to define the Bayesian estimator $E(\theta|x_1, x_2, \ldots, x_n)$ of each parameter given a sample mean $\bar{x}$.

Table 3 shows the lower and upper bounds of design variables which have been used in the analysis.

The values in Table 3 come from 770 values that have been collected. These data have been used to calculate the sample mean $\bar{x}$, the variance $\sigma_0^2$ and the lower and upper bound that is the minimum and maximum value for each variable, respectively.

## 5 Calculations and Results

The analysis is carried out in three consecutive parts. For the first part, Eqs. (1)–(7) are iterated step-by-step by using the programming language Wolfram Mathematica (2017). The equations were written in the software and then implemented. The second part comprises the definition of the Bayesian distribution. In the third part, the dam's model optimization by computing the area and the volume defined in Eqs. (15) and (16) is carried out.

**Table 3** Data collection for design variables

| Design variables | Lower bound (m) | Upper bound (m) | Sample mean, $\bar{x}$ (m) | Known variance $\sigma_0^2$ (m) |
|---|---|---|---|---|
| $t_1$ | 3.10 | 11.899 | 6.3829 | ±4.2946 |
| $t_2$ | 8.00 | 16.47 | 12.970 | ±4.0529 |
| $t_3$ | 12.00 | 35.00 | 28.6914 | ±35.8487 |
| $r_{US1}$ | 100.00 | 151.126 | 114.882 | ±151.6418 |
| $r_{US2}$ | 61.104 | 95.32 | 86.7811 | ±55.0925 |
| $r_{US3}$ | 20.377 | 42.02 | 37.0193 | ±28.2575 |
| $r_{DS1}$ | 50.299 | 125.07 | 101.6330 | ±192.5373 |
| $r_{DS2}$ | 40.005 | 90.16 | 78.7524 | ±108.7965 |
| $r_{DS3}$ | 20.084 | 40.6737 | 33.6036 | ±19.2765 |
| $s$* | 0.0477 | 0.36 | 0.2598 | ±0.0048 |
| $\beta$* | 0.50 | 1.00 | 0.7864 | ±0.0271 |

*This value is a dimensional

About the constraints, only some of them are strictly considered: the constraints that refer to Eqs. (9)–(13). The choice about using only these constraints is due to the fact that the focus of this paper is to define the dam optimum shape considering only its geometry and stability.

Figures 5, 6, 7 and 8 show the Gaussian distribution under the Bayesian hypothesis. The figures show the Bayesian estimators (vertical dashed line), PDF a priori without and with the positive variance and PDF a posteriori.

The sharpened shape of the PDF a posteriori depends of the number of samples that are used; i.e. the lesser the samples, the lower the curve is. A sharpened shape indicates that the standard deviation is low; therefore, the data tend to be close to the mean and so the estimation has a good calibration. In this analysis, 34 samples $\{x_n | n = 34\}$ for each variable have been used.

Table 4 shows the results of the Bayesian stochastic analysis. It is possible to see an existing dam's change of volumes to obtain the optimum dam: prior distribution for existing dams $\theta \sim N\ (\mu,\ \sigma^2) \rightarrow$ posterior distribution for optimized dams $\theta \sim N\left(\mu_{\mathrm{p}}, \sigma_{\mathrm{p}}^2\right)$. The last three columns of

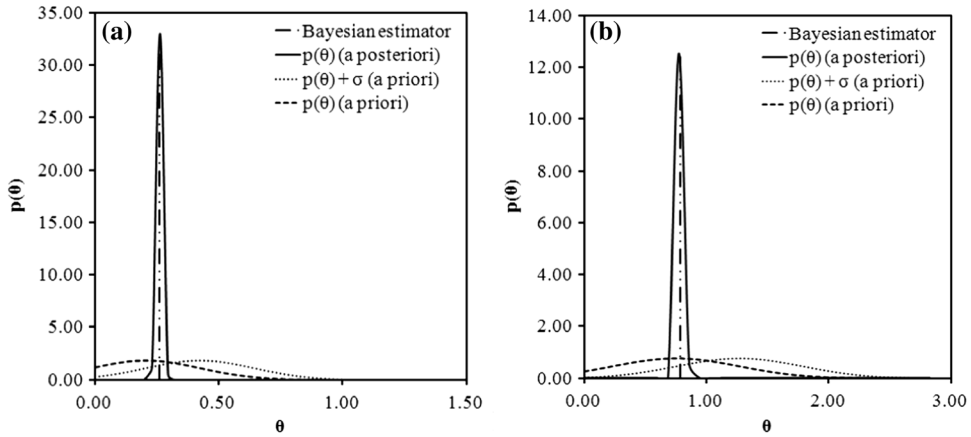


**Fig. 5** Gaussian distribution by using the Bayesian method of $s$ (**a**) and $\beta$ (**b**)

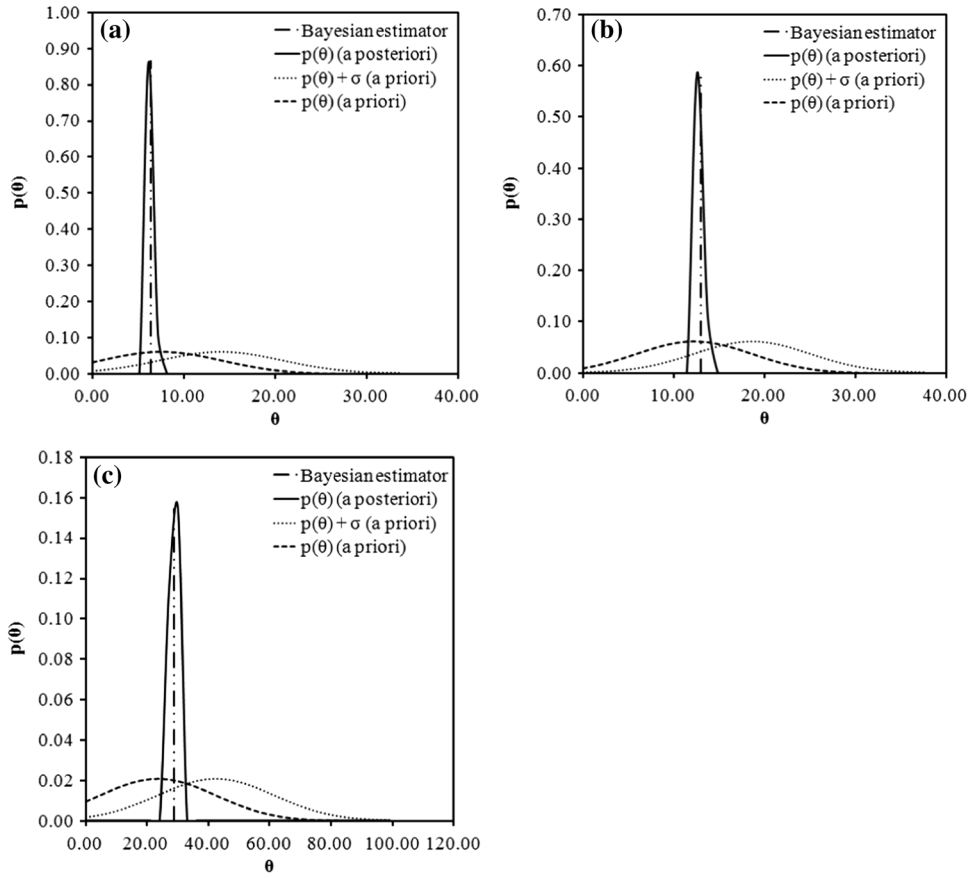


**Fig. 6** Gaussian distribution by using the Bayesian method of $t_1$ (**a**), $t_2$ (**b**) and $t_3$ (**c**)

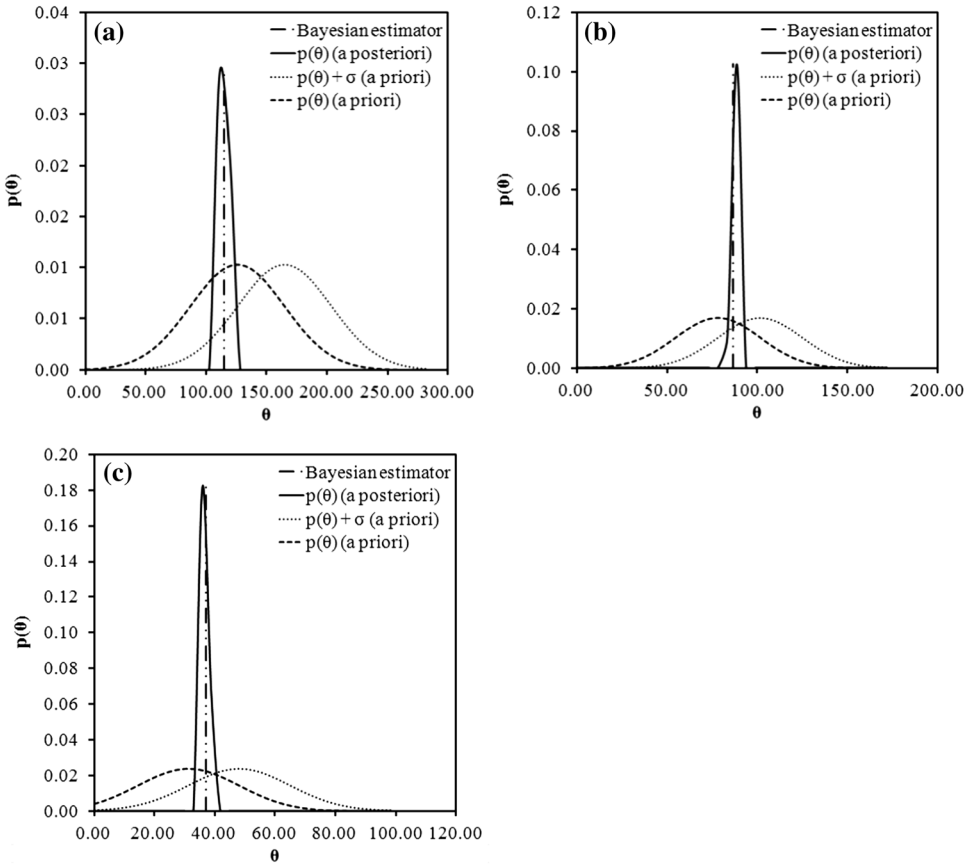


**Fig. 7** Gaussian distribution by using the Bayesian method of $r_{US1}$ (**a**), $r_{US2}$ (**b**) and $r_{US3}$ (**c**)

Table 4 show the interval that contains $\mu_p$ for a probability of 90, 95 and 99%.

The variance describes the uncertainty in the predictions of the optimal model. These values are much more plausible than any other values. The underlined values are used to design the dam.

From the posterior distribution values, the radius of the dam axis at top level is $r_{a1} = 111.7$ m and $l_a = 186.2$ m. The variance of the prior distribution has been used ten times more than the known variance. This is because the uncertainty of the prior distribution is obviously high. To respect the stability constraints, a 110° central angle of dam is considered to estimate the crest lengths to run the analysis. The lengths of the dam calculated with respect to the dam axis $l_{c1}$, $l_{c2}$, $l_{c3}$ are 215 m, 155 m, 45 m, respectively.

Figure 9 shows the mean section of the optimum shape of the dam for each level. The distance between the US and DS surfaces represents the thickness.

Table 5 shows the optimum volume and area for the three sections for the dam.

The available achievements and practical engineering applications show that optimization design can reduce the concrete volume. Concerning the dam with similar characteristic—for example, the Albarellos Dam—the concrete volume is reduced around 22% and this reduction provides advantages in terms of economic and social benefit. In this sense, the slenderness coefficient introduced by Fanelli and Lombardi (1992) and cited more recently by Hariri-Ardebili et al. (2016) as $\text{area}^2/(\text{volume} \times \text{height}) = 30152^2/(170052.40 \times 95.55) = 55.95$ indicates that the optimized arch dam is very slender and this is also due to the fact that the structure is a double-arch dam and not a gravity arch dam.

It is important to mention that the intention of the authors is not to provide these calculated variables to derive conclusions about a full shape optimization analysis.

## 6 Conclusions

The shape design is a key problem in the modelling of double-arch dams, and it is usually established based on engineering experience. Also, there are some limitations imposed by topographic conditions and foundation requirements. For instance, the largest central practicable angle should be used considering that the foundation topography may be inaccurately mapped and that the arch abutments may need to be extended to deeper excavation than originally planned.

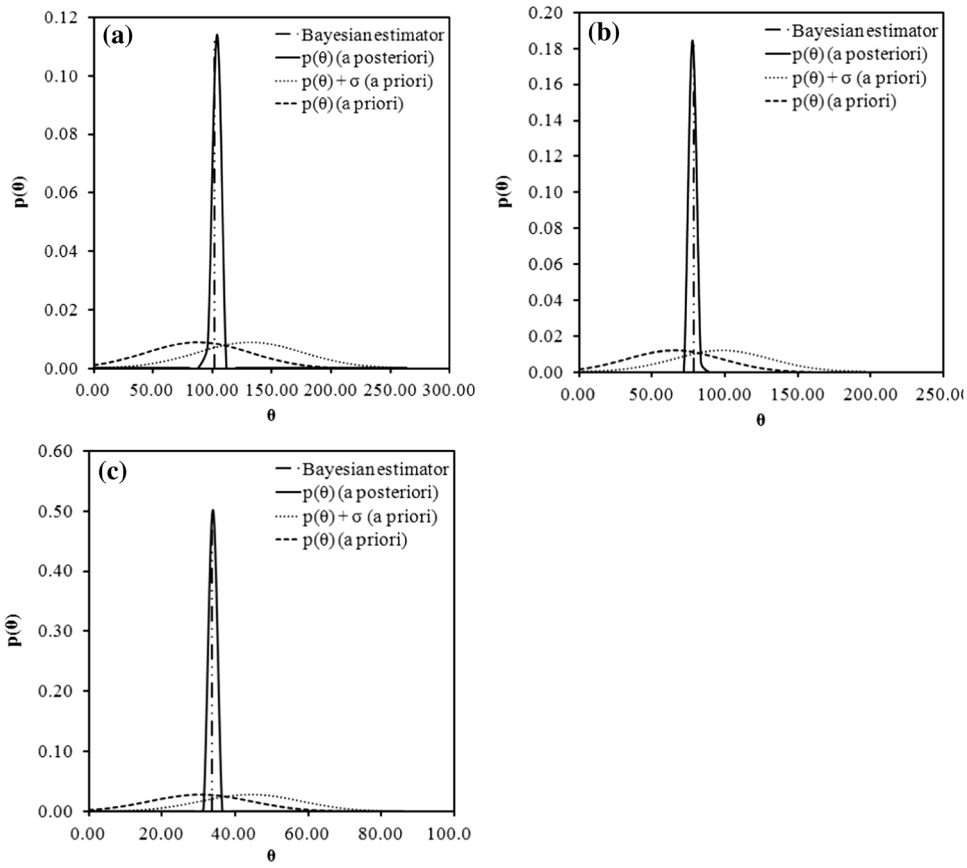


**Fig. 8** Gaussian distribution by using the Bayesian method of $r_{DS1}$ (**a**), $r_{DS2}$ (**b**) and $r_{DS3}$ (**c**)

**Table 4** Results of the Bayesian stochastic analysis

| Design variables | Existing dams prior distribution: $\theta \sim N(\mu, \sigma^2)$ | | Optimized dams posterior distribution: $\theta \sim N\left(\mu_p, \sigma_p^2\right)$ | | Interval of $\mu_p$ with a probability of: | | |
|---|---|---|---|---|---|---|---|
| | Mean value (m) | Variance (m) | Mean value (m) | Variance (m) | 90% | 95% | 99% |
| $t_1$ | 7.4995 | ±42.95 | 6.3862 | ±0.1259 | (5.80, 6.97) | (5.69, 7.08) | (5.47, 7.30) |
| $t_2$ | 12.235 | ±40.53 | 12.9678 | ±0.1189 | (12.40, 13.53) | (12.29, 13.64) | (12.08, 13.86) |
| $t_3$ | 23.50 | ±358.49 | 28.6762 | ±1.0513 | (26.99, 30.36) | (26.67, 30.68) | (26.03, 31.32) |
| $r_{US1}$ | 125.563 | ±1516.42 | 114.9133 | ±4.4470 | (111.44, 118.38) | (110.78, 119.05) | (109.47, 120.35) |
| $r_{US2}$ | 78.2120 | ±550.93 | 86.7560 | ±1.6156 | (84.66, 88.85) | (84.26, 89.25) | (83.48, 90.03) |
| $r_{US3}$ | 31.1985 | ±282.58 | 37.0022 | ±0.8287 | (35.50, 38.49) | (35.22, 38.79) | (34.65, 39.35) |
| $r_{DS1}$ | 87.6845 | ±1925.37 | 101.5921 | ±5.6463 | (97.68, 105.50) | (96.93, 106.25) | (95.46, 107.72) |
| $r_{DS2}$ | 65.0825 | ±1087.97 | 78.7123 | ±3.1905 | (75.77, 81.65) | (75.21, 82.21) | (74.10, 83.32) |
| $r_{DS3}$ | 30.3789 | ±192.77 | 33.5941 | ±0.5653 | (32.36, 34.83) | (32.12, 35.07) | (31.65, 35.53) |
| $s$* | 0.2039 | ±0.05 | 0.2596 | ±0.0001 | (0.24, 0.28) | (0.24, 0.28) | (0.23, 0.29) |
| $\beta$* | 0.75 | ±0.27 | 0.7863 | ±0.0008 | (0.74, 0.83) | (0.73, 0.84) | (0.71, 0.86) |

*This value is a dimensional. All values respect the design constraints defined in previous section for both prior and posterior distribution, for example $r_{US1} \geq r_{DS1}$, $r_{US2} \geq r_{DS2}$, $r_{US3} \geq r_{DS3}$, $3.10 \leq t_1 \leq 11.9$, $8.0 \leq t_2 \leq 16.5$, $12.0 \leq t_3 \leq 35.0$, $t_3 \geq t_2 \geq t_1$, $s \leq 0.36$, $\beta \leq 1.0$

Due to the development of innovative constructive technologies, the dam shape becomes higher, thinner and flatter. If the dam becomes flatter, the stability, related to sliding of the dam–abutment interface, increases to the advantage of the structural safety.

The difficulties at evaluating many design variables, mathematical functions and constraint conditions have been solved in this paper by the step-by-step integration and by using Bayesian estimators.

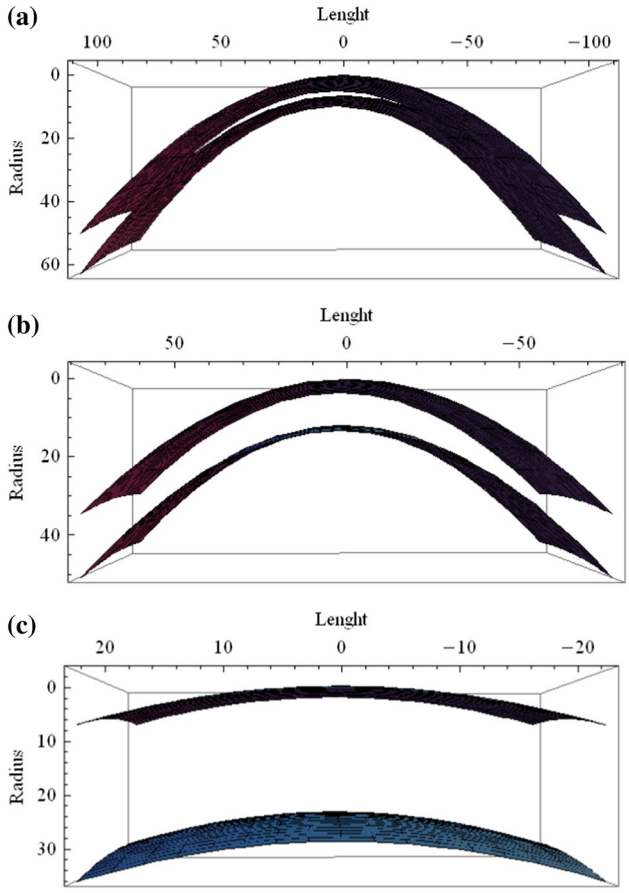


**Fig. 9** Shape of the dam horizontal sections for: **a** $63.70 \le h_1 \le 95.55$ m and $0 \le l_{c1} \le 215$ m; **b** $31.85 \le h_2 \le 63.70$ m and $0 \le l_{c2} \le 155$ m; **c** $0 \le h_3 \le 31.85$ m and $0 \le l_{c3} \le 45$ m

**Table 5** Lower and upper bounds of design variables

| Height range (m) | Length range (m) | Volume ($m^3$) | Area ($m^2$) |
|---|---|---|---|
| $63.70 \le h_1 \le 95.55$ | $0 \le l_{c1} \le 215$ | 58,780.8 | 15,820.5 |
| $31.85 \le h_2 \le 63.70$ | $0 \le l_{c2} \le 155$ | 69,839.9 | 11,256.0 |
| $0 \le h_3 \le 31.85$ | $0 \le l_{c3} \le 45$ | 41,431.7 | 3075.5 |
| Total | 17,0052.4 | 30,152.0 | |

The main conclusions drawn from this research are described as follows: (1) it is necessary to develop a more complete inventory of dams in Spain. In this sense, the competent authority must be solicited; (2) the shape optimization process requires careful data availability of existing dams; and (3) the cost of arch dams is mainly dependent on the volume of the dam body, and if the volume decreases, consequently the deadweight and stresses decrease. Moreover, a lower volume serves to better preserve the environment; (4) Bayesian theorem is well suited to a problem that comprises many variables. With many available data and a relatively small number of prediction-error parameters, the probability of a good result can be well calibrated. When parameters are unknown, it is possible to use a normal distribution that can represent the hypothesis a priori about the mean of the distribution.

From 770 collected values, 66 values are defined (Table 3 + first two columns of Table 4) to obtain 11 Bayesian estimators (third column of Table 4). The obtained optimum dam has a concrete volume reduction of 1.28 respecting the dam with similar characteristic, and 1.39 in relation to the mean volume calculated from all the selected dams. Moreover, the slender double-arch dam (ideal dam) is defined, respecting the geometric and stability constraints.

The results of this research are coherent; however, it should be mentioned that many other choices and factors should be considered to design an optimum dam. Those factors, among others, can be characteristics of foundation, type of soil, a structure body performance evaluation, adequate simulation analysis and geo-mechanical model tests, or feedback analysis of monitoring data. Finally, it is also necessary to evaluate the stability of dam's body and its foundation, once the optimization is developed. These aforementioned aspects have not been included in this paper, and they are under research.

**Acknowledgements** The first author acknowledges the "Servicios Informáticos CPD" of the University of Salamanca for the Wolfram Mathematica license and the University of Salamanca to pay the rights (when applicable) to completely download all papers in the references.

## References

Akbari A, Taghi Ahmadi M, Moharrami H (2011) Advances in concrete arch dams shape optimization. Appl Math Model 35:3316–3333. https://doi.org/10.1016/j.apm.2011.01.020

Alrarejos-García L, Escuder-Bueno I, Morales-Torres A (2015) Advances on the failure analysis of the dam-foundation interface of concrete dams. Materials 8:8255–8278. https://doi.org/10.3390/ma8125442

AutoCAD (2010) Version 2010. Autodesk, Inc

Baker JW, Gupta A (2016) Bayesian treatment of induced seismicity in probabilistic seismic-hazard analysis. Bull Seismol Soc Am 106:860–870. https://doi.org/10.1785/0120150258

Bartoli G, Betti M, Facchini L, Marra AM, Monchetti S (2017) Bayesian model updating of historic masonry towers through dynamic experimental data. Proc Eng 199:1258–1263. https://doi.org/10.1016/j.proeng.2017.09.267

Beck JL, Katafygiotis LS (1998) Updating models and their uncertainties. I: Bayesian statistical framework. J Eng Mech 124:455–461. https://doi.org/10.1061/(ASCE)0733-9399(1998)124:4

Buffi G, Manciola P, De Lorenzis L, Cavalagli N, Comodini F, Gambi A, Gusella V, Mezzi M, Niemeier W, Tamagnini C (2017a) Calibration of finite element models of concrete arch-gravity dams using dynamical measures: the case of Ridracoli. Proc Eng 199:110–115. https://doi.org/10.1016/j.proeng.2017.09.169

Buffi G, Manciola P, Grassi S, Barberini M, Gambi A (2017b) Survey of the Ridracoli dam: UAV-based photogrammetry and traditional topographic techniques in the inspection of vertical structures.

Geomat Nat Hazard Risk 8:1–18. https://doi.org/10.1080/19475705.2017.1362039
Cardarelli E, Cercato M, Di Filippo G (2010) Geophysical investigation for the rehabilitation of a flood control embankment. Near Surf Geophys 8:287–296. https://doi.org/10.3997/1873-0604.2010018
Cardarelli E, Cercato M, De Donno G (2014) Characterization of an earth-filled dam through the combined use of electrical resistivity tomography, P- and SH-wave seismic tomography and surface wave data. J Appl Geophys 106:87–95. https://doi.org/10.1016/j.jappgeo.2014.04.007
Conte JP, Astroza R, Ebrahimian H (2015) Bayesian methods for nonlinear system identification of civil structures. MATEC Web Conf 24:1–7. https://doi.org/10.1051/matecconf/20152403002
Fan Q, Zhou S, Yang N (2015) Optimization design of foundation excavation for Xiluodu super-high arch dam in China. J Rock Mech Geotech Eng 7:120–135. https://doi.org/10.1016/j.jrmge.2015.03.001
Fanelli M, Lombardi G (1992) On the Lombardi "slenderness coefficient" for assessing the cracking potential of arch dams. In: Proceeding of the international symposium on arch dams, Nanjing, China, pp 1–6
Gholizadeh S, Seyedpoor SM (2011) Shape optimization of arch dams by metaheuristics and neural networks for frequency constraints. Sci Iran 18:1020–1027. https://doi.org/10.1016/j.scient.2011.08.001
Gu H, Wu Z, Huang X, Song J (2015) Zoning modulus inversion method for concrete dams based on chaos genetic optimization algorithm. Math Probl Eng 2015:1–9. https://doi.org/10.1155/2015/817241
Hamidian D, Seyedpoor SM (2010) Shape optimal design of arch dams using an adaptive neuro-fuzzy inference system and improved particle swarm optimization. Appl Math Model 34:1574–1585. https://doi.org/10.1016/j.apm.2009.09.001
Hariri-Ardebili MA, Fugani L, Meghella M, Saouma VE (2016) A new class of seismic damage and performance indices for arch dams via ETA method. Eng Struct 110:145–160. https://doi.org/10.1016/j.engstruct.2015.11.021
IGN-UPM (2013) Actualización de Mapas de Peligrosidad Sísmica de España 2012. Editorial Centro Nacional de Información Geográfica, Madrid, p 267. ISBN 978-84-416-2685-0
Inventory of Dams and Reservoirs (2017) SNCZI. http://sig.mapama.es/snczi/visor.html. Accessed 2017
Jin F, Chen Z, Wang J, Yang J (2010) Practical procedure for predicting non-uniform temperature on the exposed face of arch dams. Appl Therm Eng 30:2146–2156. https://doi.org/10.1016/j.applthermaleng.2010.05.027
Kaveh A, Ghaffarian R (2014) Shape optimization of arch dams with frequency constraints by enhanced charged system search algorithm and neural network. Int J Civ Eng 13:102–111. https://doi.org/10.22068/IJCE.13.1.102
Khatibinia M, Khosravi Sh (2014) A hybrid approach based on an improved gravitational search algorithm and orthogonal crossover for optimal shape design of concrete gravity dams. Appl Soft Comput 16:223–233. https://doi.org/10.1016/j.asoc.2013.12.008
Khosravi S, Heydari MM (2013) Modelling of concrete gravity dam including dam-water-foundation rock interaction. World Appl Sci J 22:538–546. https://doi.org/10.5829/idosi.wasj.2013.22.04.551
Li Z, Gu C, Wu Z (2013) Nonparametric change point diagnosis method of concrete dam crack behavior abnormality. Math Probl Eng 2013:1–13. https://doi.org/10.1155/2013/969021
Li Y, Wang J, Xu Z (2016) Design optimization of a concrete face rock-fill dam by using genetic algorithm. Math Probl Eng 2016:1–11. https://doi.org/10.1155/2016/4971048
Permanent Committee of Seismic Resistant Codes (2002) NCSE-02. Seismic resistant construction code: general rules and rules for buildings. Spain
Reinoso J, Gonçalves JE, Pereira C, Bleninger T (2017) Cartography for civil engineering projects: photogrammetry supported by unmanned aerial vehicles. Iran J Sci Technol Trans Civ Eng. https://doi.org/10.1007/s40996-017-0076-x
Ridolfi E, Buffi G, Venturi S, Manciola P (2017) Accuracy analysis of a dam model from drone surveys. Sensors 17:1777–1796. https://doi.org/10.3390/s17081777
Ross SM (2008) Probability and statistics for engineers and scientists, 2nd edn. Apogeo Editor, Italy, p 614
Saber Mahani A, Shojaee S, Salajegheh E, Khatibinia M (2015) Hybridizing two-stage meta-heuristic optimization model with weighted least squares support vector machine for optimal shape of double-arch dams. Appl Soft Comput 27:205–218. https://doi.org/10.1016/j.asoc.2014.11.014
Savage JL, Houk IE (1931) Checking arch dam designs with models. Civ Eng 1:695–699. https://doi.org/10.1007/978-1-4615-4601-6_6
Seyedpoor SM, Gholizadeh S (2008) Optimum shape design of arch dams by a combination of simultaneous perturbation stochastic approximation and genetic algorithm methods. Adv Struct Eng 11:501–510. https://doi.org/10.1260/136943308786412069
Seyedpoor SM, Salajegheh J, Salajegheh E (2010) Shape optimal design of arch dams including dam-water-foundation rock interaction using a grading strategy and approximation concepts. Appl Math Model 34:1149–1163. https://doi.org/10.1016/j.apm.2009.08.005
Seyedpoor SM, Salajegheh J, Salajegheh E, Gholizadeh S (2011) Optimal design of arch dams subjected to earthquake loading by a combination of simultaneous perturbation stochastic approximation and particle swarm algorithms. Appl Soft Comput 11:39–48. https://doi.org/10.1016/j.asoc.2009.10.014
Shouyi L, Lujun D, Lijuan Z, Wei Z (2009) Optimization design of arch dam shape whit modified complex method. Adv Eng Soft 40:804–808. https://doi.org/10.1016/j.advengsoft.2009.01.013
Spanish Association of Dams and Reservoirs (2017) SEPREM. http://www.seprem.es/index.php. Accessed 2017
US Army Corps of Engineers (1994) USACE. Arch dan design. Manual No. 1110-2-2201. Washington, DC
Wolfram Mathematica (2017) Version 11 Student Edition. Wolfram Research, Inc
Xiao-fei Z, Shou-yi L, Yao-long C (2009) Optimization of geometric shape of Xiamen arch dam. Adv Eng Soft 40:105–109. https://doi.org/10.1016/j.advengsoft.2008.03.013
Yuen KV (2010) Bayesian methods for structural dynamics and civil engineering. Wiley, Asia
Yuen KV, Beck JL, Katafygiotis LS (2006) Unified probabilistic approach for model updating and damage detection. J Appl Mech 73:555–564. https://doi.org/10.1115/1.2150235
Zacchei E, Molina JL (2018) Estimation of optimal area and volume for double arch-dams. MATEC Web Conf 211:1–6. https://doi.org/10.1051/matecconf/201821114002
Zhang L, Liu Y, Zhang G, Zhang S (2015) Study on real-time simulation analysis and inverse analysis system for temperature and stress of concrete dam. Math Probl Eng 2015:1–8. https://doi.org/10.1155/2015/306165
Zhu K, Gu C, Qiu J, Liu W, Fang C, Li B (2016) Determining the optimal placement of sensors on a concrete arch dam using a quantum genetic algorithm. J Sens 2016:1–10. https://doi.org/10.1155/2016/2567305